

Two distinct modes for propagation of histone PTMs across the cell cycle

Constance Alabert^{1,2,6}, Teresa K. Barth^{3,6}, Nazaret Reverón-Gómez^{1,2}, Simone Sidoli^{2,4,5}, Andreas Schmidt³, Ole N. Jensen^{2,4}, Axel Imhof³ and Anja Groth^{1,2}

¹Biotech Research and Innovation Centre (BRIC), ²Centre for Epigenetics, University of Copenhagen, Ole Maaløes Vej 5, 2200 Copenhagen, Denmark; ³Munich Centre of Integrated Protein Science and Adolf Butenandt Institute, Ludwig-Maximilians University of Munich, Schillerstrasse 44, 80336 Munich, Germany; ⁴Department of Biochemistry & Molecular Biology, University of Southern Denmark, Campusvej 55, DK-5230 Odense, Denmark

⁵Current address: Epigenetics Program, Department of Biochemistry and Biophysics, Perelman School of Medicine, University of Pennsylvania, Philadelphia, PA, 19104, USA

⁶These authors contributed equally

Correspondence: imhof@lmu.de and anja.groth@bric.ku.dk

SUPPLEMENTAL MATERIAL

List of content:

Supplemental Material and Method, related to Figure S1E, S2B and S5C

Figure S1, related to Figure 1

Figure S2, related to Figure 1

Figure S3, related to Figure 1 & 2

Figure S4, related to Figure 3

Figure S5, related to Figure 3

Figure S6, related to Figure 3

Figure S7, related to Figure 4

Supplemental Material and Methods

Cell lines and synchronization. HeLa S3 cells were grown in spinners for 8 to 9 divisions in SILAC light medium depleted for arginine and lysine (Thermo Scientific RPMI 1640 Medium) and supplemented with dialyzed FBS (#26400-036 Invitrogen), MEM non-essential amino acid mix (#11140 Invitrogen), Glutamax (#35050-038 Invitrogen), 66 mg/L of arginine and 100 mg/L of lysine (Sigma). Cells were synchronized in G1/S by single thymidine block (Sigma, 2 mM, 17 h) and released into media containing deoxycytidine (Sigma, 24 μ M). For the double SILAC labelling, the heavy medium was complemented with heavy R6 / K8 from Cambridge Isotope Laboratories. For triple-SILAC labelling, cells were released from a thymidine arrest into heavy R6 medium and 2 hours after the b-dUTP labelling washed and transferred into heavy R10 medium. Where indicated, nocodazole (Sigma, 40 μ M) was added to the cells 2 hours after b-dUTP labelling for 10, 16 or 18 hours. Where indicated, cycloheximide (Sigma, 50-200 μ g/ml) was added to the cells

2.5 min before b-dUTP labelling and during the labelling. TIG-3 fibroblasts were grown on plates in DMEM with 10 % FBS and MEM non-essential amino acid mix.

Determination of Histone H3 K27me1 and K36me1 in nascent chromatin. The previously described sample preparation generates the peptide KSAPATGGVKKPHR of histone H3.1 containing lysines K27, K36, and K37 that can be methylated. The monomethylated isoforms cannot be separated by the chromatography settings described above. In order to determine the location of the modification and quantify the monomethylation, the mass spectrometer was programmed to acquire one MS and 4 MS/MS scans for the triply and doubly charged ions of the light and heavy SILAC (K8 and R6) labeled peptide at m/z 539.31 (light_3+), 808.47 (light_2+), 549.33 (heavy_3+), and 823.50 (heavy_2+) from 40-50 min where the peptide elution was expected. For this period, the acquisition settings for the ion trap were changed from centroid to profile mode and enhanced resolution was set for all MS/MS spectra. For localization of the monomethylation, the obtained MS/MS spectra were summed up and checked manually for fragment ions of the different monomethylated isoforms. To relatively quantify monomethylation of K27 and K36, signal areas of fragment ions uniquely coding for only one of the modifications were extracted from the raw data and fragment ion intensities with more than 250 AU (arbitrary units) were accepted for further calculation. Relative abundances of both isoforms and light and heavy SILAC labeled peptides were calculated individually for each fragment ion and afterwards averaged.

Total histone extraction, digestion and mass spectrometry analysis. Total histones from TIG-3 fibroblasts were isolated by acid extraction (Fig. 4B and Supplemental Fig. S7D). After precipitation with trichloroacetic acid (TCA) histones were resuspended in 1 mM calcium acetate, 7.5 mM dithiothreitol (DTT) and 100 mM ammonium bicarbonate (pH 8.0) by vortexing. 10 μg of histones at the concentration of 0.5 $\mu\text{g}/\mu\text{l}$ were digested by adding the proteolytic enzyme Arginine-C at an enzyme:sample ratio 1:50 at room temperature overnight. Digestion was interrupted by adding 1% trifluoroacetic acid (TFA). 1 μg of sample was loaded onto a 100 μm ID x 2 cm trap column packed with Reprosil-Pur C18-AQ (3 μm ; Dr. Maisch GmbH, Germany) material coupled online with a 75 μm ID x 16 cm picofrit-analytical column packed with the same material using an Easy-nLC nanoHPLC (Proxeon, Odense, Denmark). Injection volume was set to 5 μL . The HPLC gradient was 0-34% solvent B (A = 0.1% formic acid; B = 95% acetonitrile, 0.1% formic acid) over 60 min and from 34% to 100% solvent B in 5 min at a flow-rate of 250 nL/min. LC was coupled online with a mass spectrometer triple quadrupole TSQ Vantage (ThermoFisher Scientific, Bremen, Germany). Nanoelectrospray was used with a spray voltage of 2.3 kV. No sheath, sweep, and auxiliary gasses were used, and capillary temperature was set to 270 $^{\circ}\text{C}$. TSQ Vantage was used in selected reaction monitoring (SRM) mode. Acquisition was performed with a quadrupole peak width of 0.7 and a scan time of 0.025 s for each transition. We selected three transitions for each peptide, based on which provided the most intense signal. The collision energy

adopted was the one set by default by the software Skyline (MacLean et al. 2010). Data processing and search were performed by uploading the result files in Skyline (MacLean et al. 2010) to integrate the area below the chromatographic peak for each peptide. The three transitions were used to determine the correct peak, but only the most intense transition was used for quantification. Trimethylation (mass 42.047 Da) and acetylation (mass 42.011 Da) were discriminated by using the retention time. No discrimination could be performed for isobaric PTM combinations such as K27acK36me3 / K27me3K36ac. The relative quantification for a given peptide was obtained by dividing its quantification by the sum of all quantifications of all peptides sharing the same amino acid sequence. The mass spectrometry raw data are available upon request.

Primary antibodies. PCNA (Abcam ab29, clone PC10, 1:1000), H4K5ac (Abcam ab51997, clone EP1000Y, 1:1000), H3K27me1 (Upstate Millipore 07-448, 1:500), H3K27me3 (CST 9756, 1:500), Histone H3 (Abcam ab10799, clone Abcam 10799, 1:2000).

Histone turnover. The percentage of R10-labeled histones at 10 hours for the peptide H4 46-55 was calculated using NCC triple SILAC experiments. R10 medium was added after 2 hours and, as there is no replication, the R10 incorporation at 10 hours reflects histone turnover over 8 hours. Estimated histone turnover per hour (%) = % of R10 at 10h / 8h of R10-labeling.

Supplementary Figure Legends

Figure S1. (A) Outline of nascent chromatin capture (NCC) technology. (B) NCC pull-down and input material analyzed by western blot. Nascent chromatin was isolated immediately after b-dUTP labelling (0 h) or after 2 hours chase (2 h). (-) no b-dUTP. (C) Values for all the modifications identified from Figure 1C. The mean of 9 independent biological experiments is shown (n=9) Error bars, s.d. in brackets. Right columns, histone PTMs in Asf1 complexes identified by mass spectrometry from (Jasencakova et al. 2010), and values for all the modifications identified in the input material (whole genome). *, K27/K36me1 resolved in Figure S1E and F. ** no MS2, identification based on retention time shift and MS1. (D) Comparison of histone PTMs on old histones in nascent and total chromatin. Only marks that differ significantly are labeled. Mean is shown, n=9. Unpaired *t*-test: ***, $P < 0.001$. Values for all the modifications identified are listed in Figure S1C. (E) Distribution of H3K27me1 and H3K36me1 on old and new histones in nascent chromatin. MS/MS-based quantification of H3 mono-methylation based on signal areas of site determining fragment ions for methylation of K27 and K36 isolated from nascent chromatin as in Figure 1C. (F) Example spectrum for the monomethylated histone H3.1 peptide demonstrating signals for K27 and K36 mono-methylation. Inlets I, II, and III of fragment ions b3, y8 and y11 demonstrate the higher abundance of K27 mono-methylation as compared to K36 mono-methylation. B3 methylation (b3+Me(1)) directly shows mono-methylation of K27, whereas y8 and y11

methylation (y8+Me(1) and y11+Me(1)) result from K36 methylation and unmodified K27. The b3+ fragment ion corresponds to unmethylated K27; y8+ and y11+ to unmethylated K36/K37.

Figure S2. Cycloheximide treatment reveals that H3K27me1 is present on new histones. **(A)** Proportion of new and old histones in nascent chromatin with and without cycloheximide (CHX) treatment. **(B)** Histone marks analyzed by western blotting of NCC pull-downs from +/- CHX treated cells. Newly replicated DNA was labeled with b-dUTP for 15 min in asynchronous cells. CHX (200ug/ml) was added 2.5 min prior to b-dUTP labeling and included during labeling. PCNA and histone H3 are shown as controls (Alabert et al. 2014; Mejlvang et al. 2014). 2x indicated double the amount of sample loaded in 1x. **(C)** Experimental design for comparison of +/- CHX (50ug/ml) treated nascent chromatin. Cells were synchronized by thymidine and released in heavy SILAC medium. Newly replicated DNA was labeled with b-dUTP in the presence or not of CHX and isolated by NCC. **(D)** Proportion of new histones on newly replicated DNA shown relative to untreated control. **(E)** Modifications on histones assembled on newly replicated DNA. The mean of three independent experiments with standard deviation is shown. * P=0.022 (one sample t-test). Note: By western-blot, the amount of parental histones loaded between the two conditions is similar; therefore the level for parental PTMs is unchanged by CHX treatment. By mass spectrometry, the percentage of the modifications depends on the proportion of new and old histones. In CHX, the proportion of old histones increase compares to new histones, therefore the level for parental PTMs will increase.

Figure S3. **(A)** Experimental design for analyzing nascent chromatin from early and late replicating regions. **(B, C)** Comparison of histone PTMs on new (b) and old (c) histones in nascent chromatin isolated in early or late S phase. The mean of 3 independent biological experiments is shown (n=3). Only marks that differ significantly are labeled (Unpaired *t*-test, H4 2ac, P= 0,0292; H3K27/36me1, P= 0,0032; H4K20me2, P= 0,0034). **(D)** Values for all PTMs identified in (b, c). Error bars, s.d. in brackets. Boxed values indicate significant differences between early and late S phase. **(E)** Enrichment of old H3.3, H2A.X and H2A.Z relative to total old histone H3 (H3.3 + H3.1/2) and histone H2A (H2A + H2A.Z + H2AX), respectively. E, early S phase; M, middle S; L, late S phase. **(f)** Enrichment of new H3.3, H2A.X and H2A.Z relative to total new histone H3 (H3.3 + H3.1/2) and histone H2A (H2A + H2A.Z + H2AX), respectively.

Figure S4. **(A)** Experimental design of the time-course analysis by double-SILAC. Nascent chromatin was labeled as in Figure 1A and maturation of b-dUTP labeled chromatin was followed as cells progress through mitosis and into G1 phase. **(B-D)** Modifications on new and old histone H3 and H4 in b-dUTP labeled chromatin. All peptides carrying the indicated modification were counted (including combination with other marks). Error bars, s.d. n≥3. **(E)** Additional PTMs on new and old histones

H4 and H3 in b-dUTP labeled chromatin analyzed by double-SILAC. Error bars, s.d. in brackets, $n \geq 3$.

Figure S5. (A) Design of pulsed triple-SILAC time-course analysis. Nascent chromatin was labeled as in Figure 1A and maturation of b-dUTP labeled chromatin was followed as cells divide and progress through subsequent cell cycles. (B) Design of pulsed triple-SILAC experiment to follow modifications of new histones from generation 1 through more than one cell cycle. (C) Proportion of old histones generation 1 (orange), new histones generation 1 (blue) and new histones generation 2/3 (grey) in b-dUTP labeled chromatin, isolated after one (0 h, nascent; 10 h, G1), two (24 h) and three (48 h) rounds of replication. Thin lines on the right indicate the theoretical proportions after one (0 and 10 h), two (24 h) and three (48 h) rounds of replication. Histone turnover was estimated on the basis of histone H4 R10-labelling at 10 hours, which represent replication-independent incorporation (see material & methods). (D) Kinetics of PTM restoration as shown in Figure 3A. The total PTM level on replicated DNA (green) is compared to the PTM level of the old histones alone, which in nascent chromatin represents the parental chromatin state (P, orange). Error bars, s.d. $n \geq 3$. Unpaired *t*-test identified differences from the parental state.

Figure S6. (A) Additional PTMs on new and old histones H4 and H3 in b-dUTP labeled chromatin analyzed by triple-SILAC. Error bars, s.d. in brackets, $n \geq 3$. (B) Dynamics of H3K9 methylation on new and old histones. Error bars, s.d. $n \geq 3$.

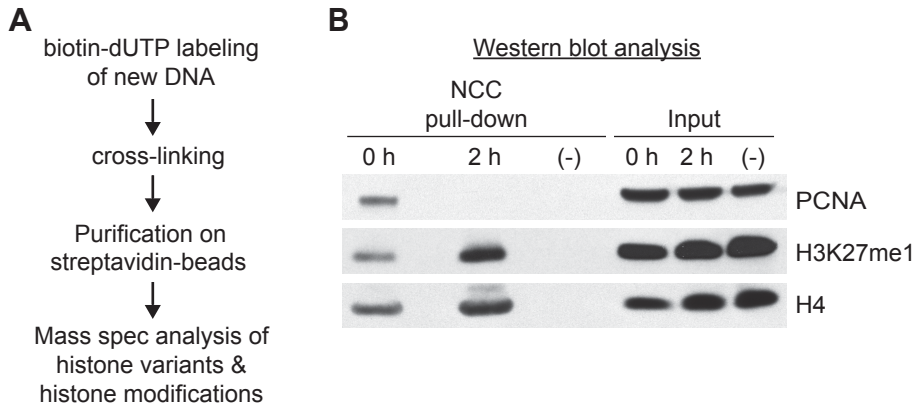
Figure S7. (A) Experimental design for nocodazole block experiment in Figure 4A. (B) H3S10 phosphorylation was increased during nocodazole arrest on both new and old histones regardless of H3K9me3. Phosphorylation therefore does not affect the conclusions drawn in Figure 4A. (C) Experimental design for cell cycle withdrawal in Figure 4B. Exponentially growing primary TIG-3 fibroblasts were harvested 24 hours after plating. Contact inhibited cells were harvested 6 days later. (D) Analysis of K79 methylation level in exponentially growing (green) and contact inhibited (purple) TIG-3 fibroblasts. Mean is shown with error bars, s.d. $n=3$. Unpaired *t*-test: **, $P < 0.01$; *, $P < 0.05$.

Alabert C, Bukowski-Wills JC, Lee SB, Kustatscher G, Nakamura K, de Lima Alves F, Menard P, Mejlvang J, Rappsilber J, Groth A. 2014. Nascent chromatin capture proteomics determines chromatin dynamics during DNA replication and identifies unknown fork components. *Nature cell biology* **16**: 281-293.

Jasencakova Z, Scharf AN, Ask K, Corpet A, Imhof A, Almouzni G, Groth A. 2010. Replication stress interferes with histone recycling and predeposition marking of new histones. *Molecular cell* **37**: 736-743.

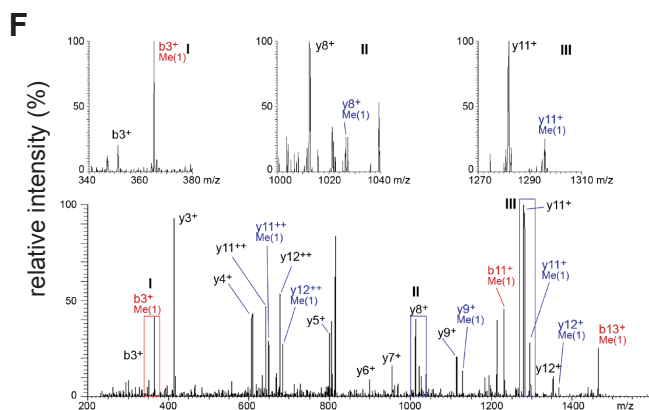
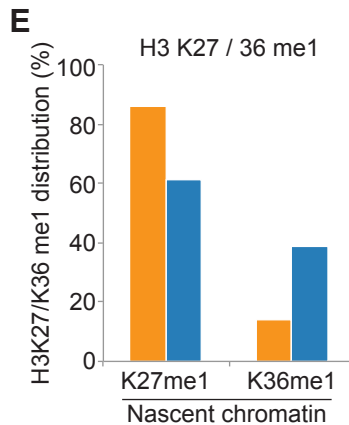
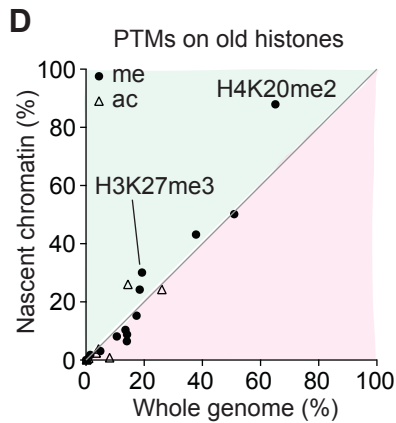
MacLean B, Tomazela DM, Shulman N, Chambers M, Finney GL, Frewen B, Kern R, Tabb DL, Liebler DC, MacCoss MJ. 2010. Skyline: an open source document editor for creating and analyzing targeted proteomics experiments. *Bioinformatics* **26**: 966-968.

Mejlvang J, Feng Y, Alabert C, Neelsen KJ, Jasencakova Z, Zhao X, Lees M, Sandelin A, Pasero P, Lopes M et al. 2014. New histone supply regulates replication fork speed and PCNA unloading. *The Journal of cell biology* **204**: 29-43.

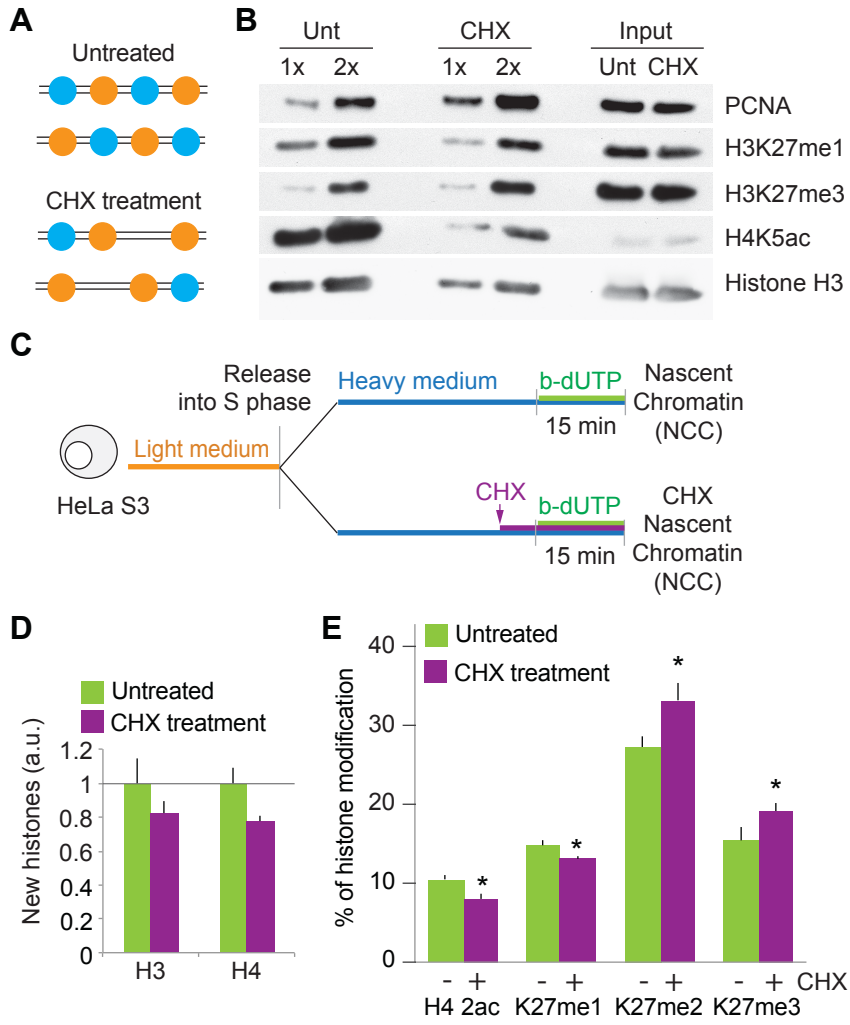


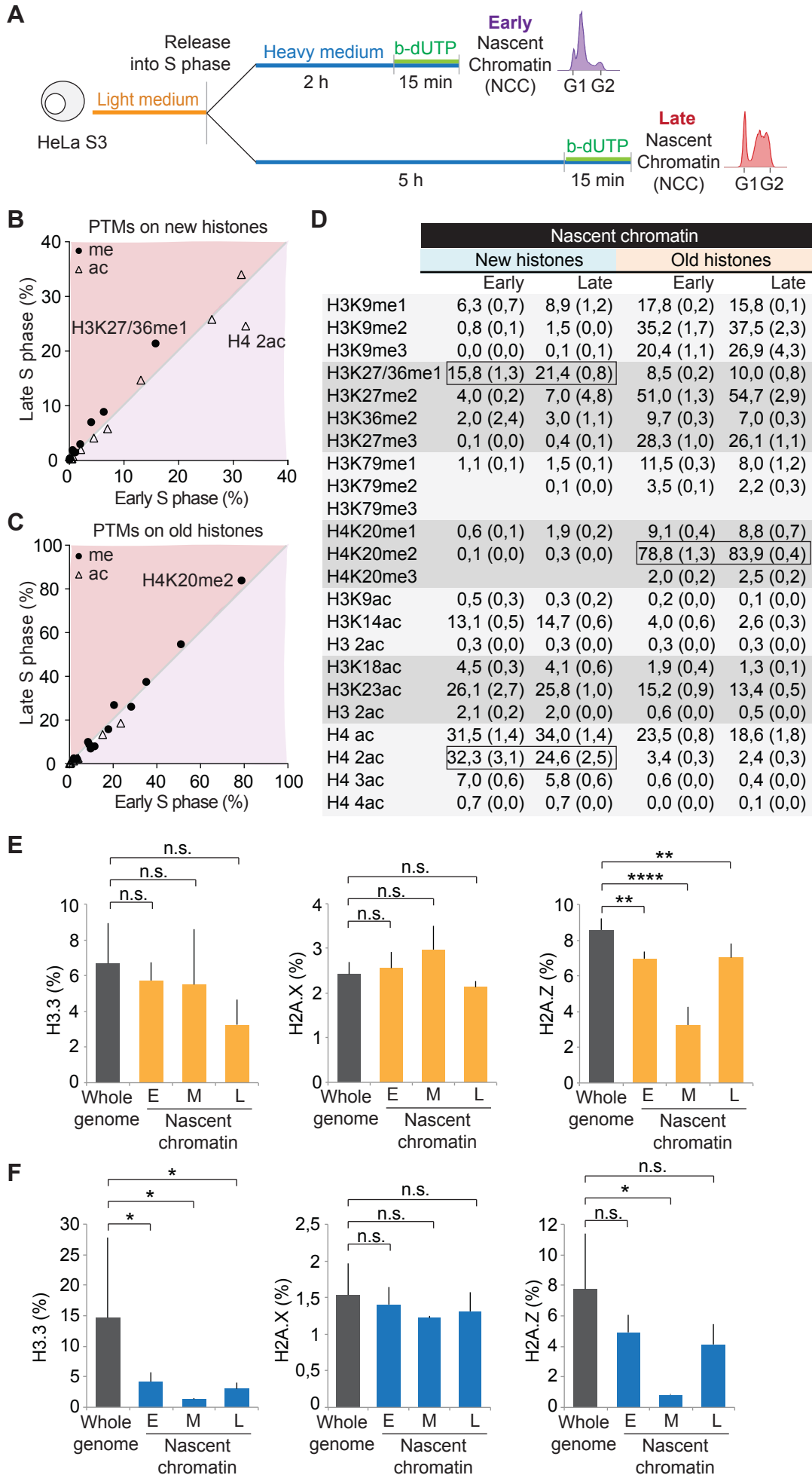
C

| | Nascent chromatin | | Soluble histones | Whole genome | |
|-----------|-------------------|-------------|--------------------|--------------|-------------|
| | Old histone | New histone | Jasencakova et al. | Old histone | New histone |
| K9me1 | 15,3 (4,2) | 4,0 (1,2) | 6,3 | 17,4 (3,5) | 8,1 (4,4) |
| K9me2 | 43,2 (5,0) | 1,2 (0,8) | 0,0 | 37,8 (6,2) | 3,9 (1,8) |
| K9me3 | 24,2 (5,0) | 0,1 (0,0) | 0,1 | 18,5 (3,3) | 0,5 (0,2) |
| K27/36me1 | 8,8 (2,5) | 12,7 (3,9) | | 14,1 (5,6) | 34,3 (1,5) |
| K27me2* | 50,2 (6,6) | 3,4 (1,9) | | 51,0 (3,8) | 10,4 (2,8) |
| K36me2* | 8,1 (6,8) | 0,6 (0,3) | | 10,6 (1,0) | 3,7 (1,5) |
| K27me3 | 30,1 (4,2) | 0,1 (0,1) | | 19,2 (4,4) | 0,3 (0,1) |
| K79me1 | 10,4 (1,6) | 0,9 (0,5) | | 13,6 (1,6) | 2,3 (0,8) |
| K79me2 | 3,1 (4,1) | 0,2 (0,2) | | 4,9 (3,1) | 0,2 (0,0) |
| K79me3 | 0,0 (0,0) | 0,5 (0,4) | | 0,0 (0,0) | 0,2 (0,1) |
| K20me1 | 6,5 (3,1) | 0,6 (0,2) | | 14,1 (7,2) | 3,5 (1,4) |
| K20me2 | 88,0 (3,0) | 2,9 (4,4) | | 65,1 (14,4) | 0,5 (0,3) |
| K20me3 | 1,8 (1,1) | 0,0 (0,0) | | 1,5 (0,4) | 0,2 (0,3) |
| K9ac | 0,5 (0,7) | 2,8 (5,5) | 23,0 | 0,3 (0,1) | 0,6 (0,2) |
| K14ac | 2,4 (0,6) | 16,5 (4,4) | | 3,5 (0,8) | 16,8 (2,3) |
| 2ac | 0,3 (0,1) | 0,2 (0,1) | | 0,4 (0,2) | 0,4 (0,1) |
| K18ac | 0,8 (0,1) | 3,8 (0,6) | 31,3 | 8,1 (10,7) | 14,4 (18,0) |
| K23ac | 26,0 (9,3) | 40,3 (6,1) | | 5,6 (6,3) | 12,7 (14,4) |
| H3K56ac** | 0,03 (0,0) | 0,01 (0,0) | 0,6 | 0,03 (0,0) | 0,5 (0,9) |
| H4 ac | 24,3 (1,6) | 29,9 (2,4) | | 26,1 (6,8) | 32,7 (4,3) |
| H4 2ac | 3,8 (0,5) | 37,0 (4,2) | | 4,3 (1,7) | 15,6 (2,9) |
| H4 3ac | 0,7 (0,2) | 11,2 (1,8) | | 0,9 (0,5) | 3,5 (0,7) |
| H4 4ac | 0,1 (0,0) | 1,1 (0,4) | | 0,2 (0,1) | 0,5 (0,1) |

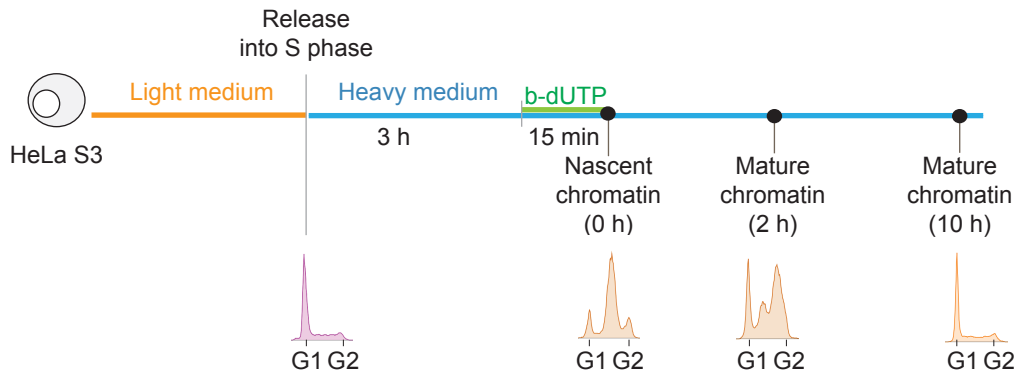


Alabert_FigS2

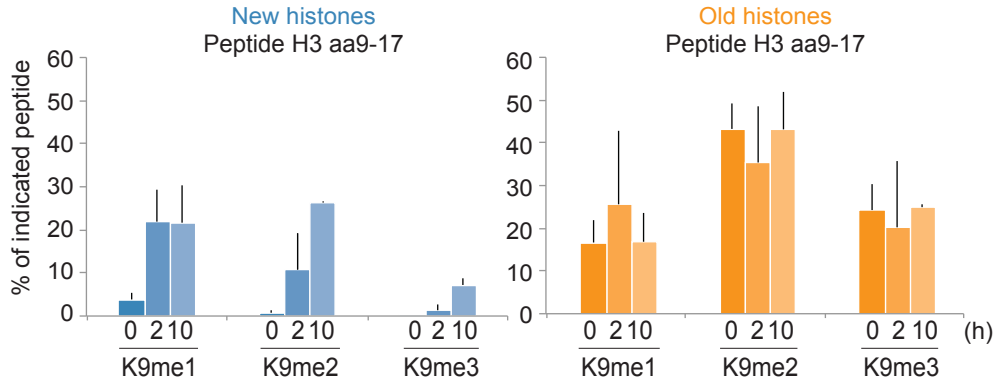




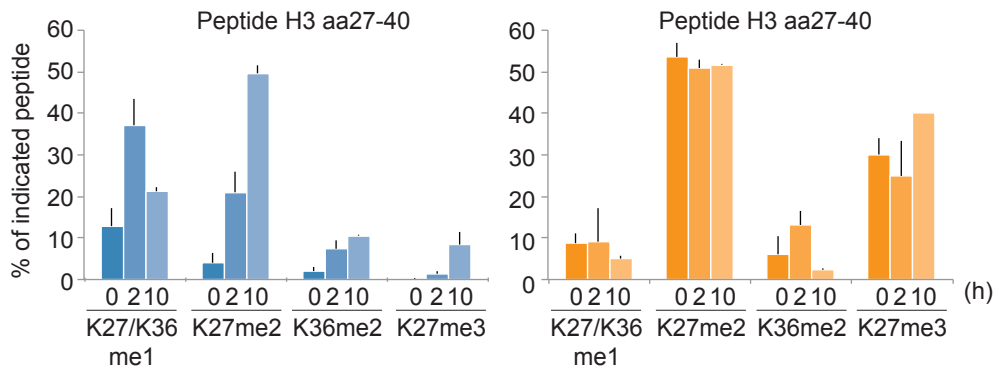
A



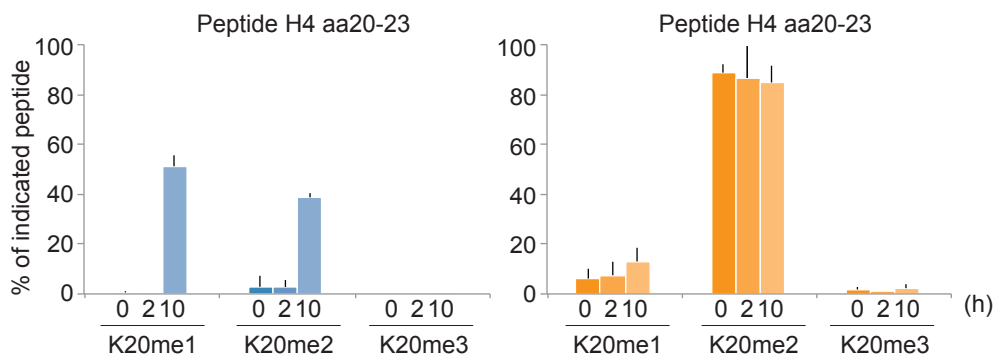
B



C

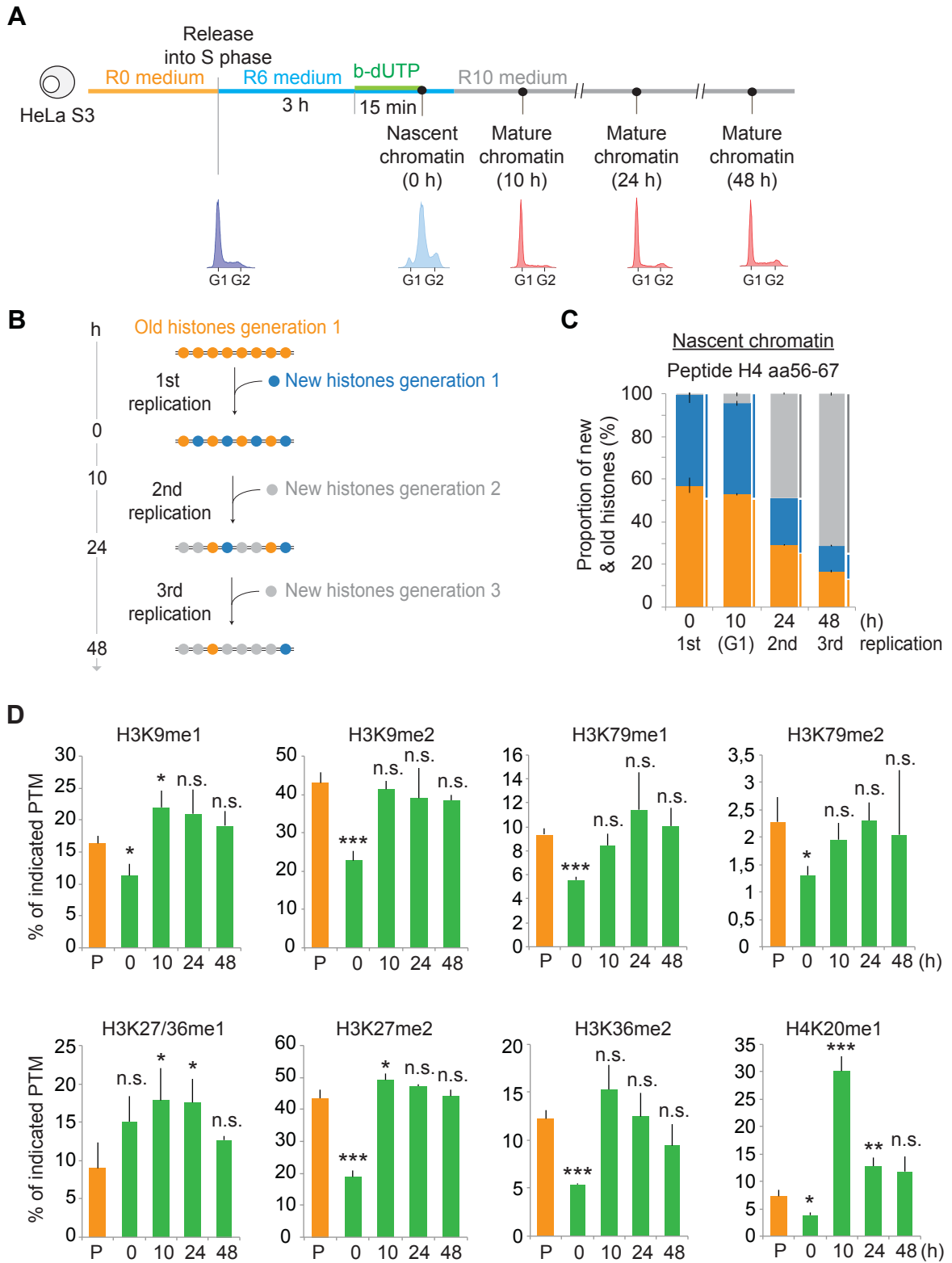


D



E

| | New histones | | | Old histones | | |
|------------|--------------|-------------|------------|--------------|-------------|------------|
| | 0h | 2h | 10h | 0h | 2h | 10h |
| H3K79me1 | 0,9 (0,6) | 1,3 (0,9) | 6,8 (1,7) | 10,9 (1,7) | 10,5 (2,8) | 14,7 (0,9) |
| H3K79me2 | 0,2 (0,2) | 0,1 (0,0) | 0,4 (0,0) | 3,6 (5,4) | 0,9 (0,5) | 2,4 (0,8) |
| H3K79me3 | 0,5 (0,4) | | 0,2 (0,0) | 0,0 (0,0) | | 0,0 (0,0) |
| H3K9ac | 0,4 (0,0) | | 0,4 (0,2) | 0,2 (0,0) | 0,2 (0,0) | 0,1 (0,0) |
| H3K14ac | 15,4 (4,7) | 11,5 (4,4) | 7,5 (0,3) | 2,3 (0,7) | 1,5 (0,9) | 2,4 (0,3) |
| H3 2ac | 0,2 (0,0) | | 0,3 (0,0) | 0,2 (0,0) | 0,1 (0,1) | 0,2 (0,0) |
| H3K18/23ac | 38,8 (8,1) | 44,8 (11,3) | 33,4 (1,8) | 22,7 (7,4) | 31,0 (10,4) | 25,4 (4,1) |
| H3 2ac | 2,8 (1,7) | 1,7 (0,6) | 1,4 (0,5) | 0,7 (0,2) | 0,7 (0,2) | 0,8 (0,2) |
| H4 ac | 29,5 (3,0) | 32,6 (0,3) | 33,0 (1,1) | 24,9 (1,7) | 26,5 (1,0) | 31,9 (1,7) |
| H4 2ac | 37,3 (5,3) | 11,4 (3,3) | 12,2 (0,4) | 3,5 (0,4) | 4,0 (1,2) | 7,2 (1,0) |



A

| | New histones | | | | Old histones | | | |
|------------|--------------|------------|------------|------------|--------------|------------|------------|------------|
| | 0h | 10h | 24h | 48h | 0h | 10h | 24h | 48h |
| H3K36me2 | 0,8 (0,3) | 18,0 (2,8) | 14,3 (3,4) | 9,9 (2,0) | 12,2 (0,9) | 12,5 (2,4) | 11,0 (2,0) | 9,1 (2,4) |
| H3K79me1 | 0,9 (0,0) | 5,4 (0,6) | 9,1 (2,6) | 8,9 (1,8) | 9,4 (0,5) | 11,1 (1,2) | 13,2 (3,4) | 10,9 (1,2) |
| H3K79me2 | 0,0 (0,0) | 0,6 (0,3) | 1,6 (0,2) | 1,8 (0,4) | 2,3 (0,4) | 3,1 (0,2) | 2,9 (0,3) | 3,4 (0,3) |
| H3K79me3 | NF | NF | NF | NF | NF | NF | NF | NF |
| H4K20me1 | 0,5 (0,0) | 46,2 (4,5) | 14,2 (2,3) | 11,2 (2,0) | 7,3 (1,2) | 14,1 (1,9) | 11,7 (1,0) | 12,1 (3,2) |
| H4K20me2 | 0,0 (0,0) | 48,7 (4,6) | 83,3 (2,9) | 87,0 (1,9) | 86,7 (2,6) | 84,8 (2,4) | 84,7 (1,7) | 84, (2,1)2 |
| H4K20me3 | 0,0 (0,0) | 0,0 (0,0) | 0,0 (0,0) | 0,0 (0,0) | NF | 1,6 (0,0) | 1,2 (0,0) | 2,2 (0,0) |
| H3K9ac | 0,7 (0,0) | 0,3 (0,0) | 0,4 (0,0) | NF | 0,2 (0,0) | 0,2 (0,0) | 0,3 (0,0) | NF |
| H3K14ac | 17,9 (0,9) | 4,1 (0,3) | 5,1 (0,5) | 4,4 (0,5) | 2,6 (0,1) | 1,8 (0,1) | 4,0 (0,6) | 4,1 (0,7) |
| H3 2ac | 0,3 (0,1) | 0,3 (0,0) | 0,4 (0,0) | 0,3 (0,0) | 0,4 (0,1) | 0,4 (0,0) | 0,9 (0,3) | 0,9 (0,2) |
| H3K18/23ac | 40,0 (1,9) | 30,6 (2,6) | 31,1 (0,8) | 27,8 (2,0) | 20,4 (1,5) | 25,0 (2,2) | 27,8 (0,2) | 26,7 (1,7) |
| H3 2ac | 2,7 (0,6) | 1,1 (0,2) | 1,0 (0,3) | 0,8 (0,6) | 2,3 (0,7) | 3,6 (0,9) | 3,7 (1,2) | 3,0 (1,8) |
| H4 ac | 30,7 (0,3) | 29,8 (1,2) | 33,6 (2,3) | 35,2 (1,9) | 23,1 (0,8) | 26,2 (2,2) | 29,8 (1,7) | 33,3 (2,4) |
| H4 2ac | 36,4 (0,1) | 7,9 (1,5) | 9,1 (1,4) | 8,6 (2,0) | 4,4 (0,1) | 5,5 (1,2) | 7,7 (1,7) | 8,1 (1,6) |

B

